

Mechanism of N-acetyl-cysteine inhibition on the cytotoxicity induced by titanium dioxide nanoparticles in JB6 cells transfected with activator protein-1

HONGBO SHI^{1,2*}, YUANLIANG GU^{1*}, ZHENHUA XIE^{3*}, QI ZHOU¹, GUOCHUAN MAO^{1,2}, XIALU LIN¹, KUI LIU¹, YU LIU¹, BAOBO ZOU¹ and JINSHUN ZHAO¹

¹Public Health Department of Medical School, Zhejiang Provincial Key Laboratory of Pathological and Physiological Technology, Ningbo University, Ningbo, Zhejiang 315211; ²Ningbo Municipal Center for Disease Control and Prevention, Ningbo, Zhejiang 315010; ³Department of Urology, Ningbo Yinzhou No. 2 Hospital, Ningbo, Zhejiang 315100, P.R. China

Received September 28, 2015; Accepted January 26, 2016

DOI: 10.3892/etm.2017.4415

Abstract. The present study investigated the mechanism of N-acetyl-cysteine (NAC) inhibition on the cytotoxicity induced by titanium dioxide (TiO₂) nanoparticles (NPs) using murine epidermal JB6 cells transfected with activator protein-1 (AP-1), JB6-AP-1 cells. Confocal microscopy was performed to localize TiO₂ NPs in cultured cells. The level of reactive oxygen species (ROS) present in cells was evaluated by staining with 2',7'-dichlorodihydrofluorescein diacetate and dihydroethidium. AP-1 gene expression levels in the cells were detected using the luciferase assay. Confocal microscopy indicated that TiO₂ NPs passed through the cell membrane into the cytoplasm; however, they did not penetrate the nuclear membrane. The present findings indicated that NAC markedly inhibited ROS generation and significantly inhibited cytotoxicity (P<0.05) induced by TiO₂ NPs. Furthermore, alternative studies have demonstrated that AP-1 luciferase activity induced by TiO₂ NPs may be significantly inhibited by NAC. In conclusion, the ability for NAC to inhibit the cytotoxicity induced by TiO₂ NPs may primarily occur by blocking ROS generation in the cultured cells.

Introduction

Nanoparticles (NPs) refer to ultrafine particles with diameter <100 nm (1). Due to their small size, the catalytic activity of

NPs is increased (2). Titanium dioxide (TiO₂) NPs possess various unique characteristics including superhydrophilic properties (3,4), energy absorption and lower transparency, which make them suitable for use in articulating prosthetic implants (5,6) sunscreens (7), biomedical fields, toothpaste (8) and textiles (9). Furthermore, previous results have supported the application of TiO₂ NPs in advanced imaging technology and medical treatments (10). TiO₂ NPs have wide applications and exposure of TiO₂ NPs may cause direct or indirect adverse health effects on the human body (11). A previous study has demonstrated that exposure to TiO₂ NPs results in an increase of reactive oxygen species (ROS) and glutathione levels in liver cells, accompanied by dose-dependent cytotoxicity (12). N-acetyl-cysteine (NAC) is a commonly used antioxidant that is used in toxicological research due to its beneficial properties, including water solubility and low toxicity (13,14). Furthermore, previous studies have demonstrated that NAC is able to prevent DNA mutations and suppress tumorigenesis (13). Additionally, previous results have demonstrated that ROS induced by zinc oxide NPs may be markedly scavenged by NAC (15). In clinical practice, NAC is used frequently as an antagonist to prevent traumatic brain injury promoted by inflammatory factors (16). In the present study, the underlying mechanism of NAC inhibition on the cytotoxicity induced by TiO₂ NPs in JB6 cells transfected with activator protein-1 (AP-1) was investigated.

Materials and methods

Materials. TiO₂ NPs (Lot No. 20110228) and fluorescein isothiocyanate (FITC)-labeled TiO₂ NPs were purchased from Hangzhou Wanjing New Material Co., Ltd. (Hangzhou, China). Characteristics of the particles are listed in Table I. Dulbecco's modified Eagle's medium (DMEM), fetal bovine serum (FBS) and trypsin were purchased from Gibco (Thermo Fisher Scientific, Inc., Waltham, MA, USA). Hoechst 33,342, 2',7'-dichlorodihydrofluorescein diacetate (H₂DCFDA) and dihydroethidium (DHE) were purchased from Invitrogen (Thermo Fisher Scientific, Inc.). The luciferase assay kit was purchased from Promega Corporation (Madison, WI, USA).

Correspondence to: Professor Jinshun Zhao, Public Health Department of Medical School, Zhejiang Provincial Key Laboratory of Pathological and Physiological Technology, Ningbo University, 818 Fenghua Road, Ningbo, Zhejiang 315211, P.R. China
E-mail: zhaojinshun@nbu.edu.cn

*Contributed equally

Key words: titanium dioxide nanoparticles, cytotoxicity, reactive oxygen species, N-acetyl-cysteine, inhibition

Table I. Characteristics of TiO₂ NPs used in the present study.

Name	Crystal form	Surface feature	Purity (%)	Particle size (nm)	Impurities (ppm)
TiO ₂ NPs	100% Anatase	Hydrophilic	99.99	40±5	Pb, <2 Cd, <1 As, <1 Hg, <1 Ni, <1

TiO₂ NPs, titanium dioxide nanoparticles; Pb, lead; Cd, cadmium; As, arsenic; Hg, mercury; Ni, Nickel.

TiO₂ NP solution preparation. Stock solutions of TiO₂ NPs were prepared by sonication on ice using a sonicator (Branson Ultrasonics, Slough, UK) in sterile PBS (10 mg/ml) for 30 sec. Prior to the experiment, the stock solution (1 µg/µl) was diluted to a desired concentration (0, 1, 5, 10, 15, 20 or 25 µg/ml) in fresh DMEM. All samples were prepared under sterile conditions.

Surface area and size distribution measurements. TiO₂ NP size distribution was determined at room temperature using scanning electron microscopy (SEM; Hitachi S-4800; Hitachi, Ltd., Tokyo, Japan). TiO₂ NPs were prepared by sonication and samples were diluted in double-distilled water (10 mg/ml). Subsequently, the samples were air-dried on a carbon planchet. Images were captured using SEM and Optimas 6.5 image analysis software (Meyer Instruments, Inc., Houston, TX, USA) was used to determine the diameter of the particles.

Cell culture. Mouse epidermal JB6 cells were obtained from the National Institute of Occupational Safety and Health (Washington, D.C., USA) and stably transfected with the AP-1 gene, as described previously (17), and cultured in DMEM supplemented with 5% FBS, 2 mM L-glutamine and 1% penicillin-streptomycin (10,000 U/ml penicillin and 10 mg/ml streptomycin) at standard culture conditions (37°C, 80% humidified air and 5% CO₂). For all treatments, cells were grown to 80% confluency.

Localization of TiO₂ NPs in culture cells. JB6-AP-1 cells were seeded in a 6-well plate (2.0x10⁵ cells in 2 ml DMEM/well) and exposed to 10 µg/cm² FITC-labeled TiO₂ NPs for 12 h at 4°C. Following two washes for 30 sec with PBS, cells were fixed in 95% ethanol for 5 min at room temperature and stained with Hoechst 33342 dye buffer for 30 min. Following two washes with PBS, particle localization in the cells was observed using a confocal microscope (magnification, x400) (Olympus Corporation, Tokyo, Japan).

ROS detection. H₂DCFDA and DHE were used for staining general ROS and oxygen radicals in cells, respectively. Hoechst staining was performed as follows and used as a nucleic acid stain to indicate the nucleus. Cells treated without TiO₂ NPs were used as a control, and H₂O₂ (200 µM) treated cells were used as a positive control. JB 6-AP-1 cells (2.0x10⁵ cells in 2 ml DMEM/well) were seeded onto a slide that had been placed in a 6-well plate. Cultures were grown for 24 h in an incubator

(37°C, 80% humidified air containing 5% CO₂) and starved in DMEM supplemented with 0.1% FBS overnight. Subsequently, cells were treated with or without TiO₂ NPs (25 µg/cm²) or TiO₂ NPs plus 40 nM NAC or 200 µM H₂O₂ in the presence of H₂DCFDA (5 µM), DHE (2 µM) and Hoechst 33342 (3 µM) for 1 h. Cells were washed for 30 sec three times with PBS and 0.1% of fresh FBS-DMEM was added. Phase contrast was used and images were captured using a fluorescence microscope (magnification, x400; LSM510; Zeiss, Germany).

MTT assay. Cell viability was assessed by the MTT assay. JB6-AP-1 cells were plated in 200 µl DMEM at a density of 10⁴ cells/well in a 96-well plate. Following a 24-h incubation period at 37°C, cells were treated with varying concentrations (0, 1, 5, 15, 20 or 25 µg/cm²) of TiO₂ NPs with or without 40 nM NAC in a phenolsulfonphthalein-free DMEM overnight (cells without any treatment were used as a control). Subsequently, cells were incubated with 10 µl MTT reagent for 4 h at 37°C. DMEM with the MTT reagent was discarded and 50 µl dimethyl sulfoxide was added. The optical density of each well was measured at a wavelength of 575 nm following shaking for 5 min.

Luciferase assay. JB6-AP-1 cells were seeded in a 24-well plate (0.5x10⁵ cells in 0.5 ml/well) and incubated for 12 h (37°C in an 80% humidified atmosphere containing 5% CO₂). Cells were starved in DMEM supplemented with 0.1% FBS overnight and subsequently exposed to different concentrations of TiO₂ NPs (0, 1, 5, 10, 15, 20 or 25 µg/cm²) with or without 40 nM NAC for 12 h. Cells without any treatments were used as a control. Luciferase activity was measured using a luciferase assay kit according to the manufacturer's instructions.

Statistical analysis. Results were expressed as the mean ± standard deviation. Statistical differences were determined using SAS 9.1.3 software (SAS Institute, Inc., Cary, NC, USA). Multiple group comparisons of the data were performed using the one-way analysis of variance test. Dunnett's test was used to compare the difference between the experimental groups and the control group. P<0.05 was considered to indicate a statistically significant difference.

Results

The average size distribution of TiO₂ NPs. The image of TiO₂ NPs was captured using SEM (Fig. 1). The average TiO₂ NP

Table II. Relative AP-1 luciferase activity.

TiO ₂ NPs ($\mu\text{g}/\text{cm}^2$)	Relative AP-1 luciferase activity	
	TiO ₂ NPs alone	TiO ₂ NPs plus 40 nM NAC
0	4775.67 \pm 740.15	6341.00 \pm 106.93
1	5052.67 \pm 811.58	5592.67 \pm 644.40
5	6955.33 \pm 930.04	3759.33 \pm 111.89 ^b
10	36521.67 \pm 9788.71 ^a	3039.67 \pm 624.69 ^b
15	57157.00 \pm 9482.12 ^a	2809.67 \pm 732.57 ^b
20	75903.00 \pm 14334.71 ^a	2464.33 \pm 528.18 ^b
25	68298.67 \pm 8077.65 ^a	5114.33 \pm 1878.85 ^b

Values are presented as mean \pm standard deviation. ^aP<0.05 vs. 0 $\mu\text{g}/\text{cm}^2$ TiO₂ NPs, ^bP<0.05 vs. TiO₂ NPs treatment alone. AP-1, activator protein 1; TiO₂ NPs, titanium dioxide nanoparticles; NAC, N-acetyl-cysteine.

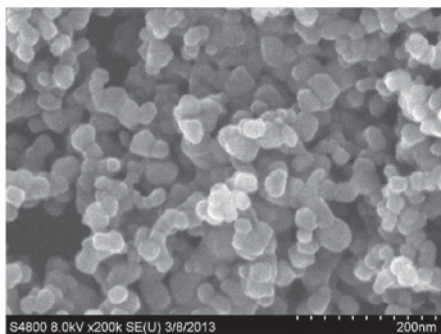


Figure 1. A scanning electron microscope was used to capture an image of titanium dioxide nanoparticles.

size distribution was 42.30 \pm 4.60 nm, which was detected by Optimas 6.5 image analysis software.

Localization of TiO₂ NPs in JB6-AP-1 cells. Following treatment with FITC-labeled TiO₂ NPs, fluorescence microscopy was performed. Hoechst 33342 was used to stain the nucleus. The captured images indicated that the TiO₂ NPs were localized in the cytoplasm and no TiO₂ NPs were present in the nucleus, which was indicated by a nuclear shadow that demonstrated no FITC-fluorescence (Fig. 2).

ROS detection. Following exposure with 25 $\mu\text{g}/\text{cm}^2$ TiO₂ NPs alone or 25 $\mu\text{g}/\text{cm}^2$ TiO₂ NPs plus 40 nM NAC, H₂DCFDA and DHE dyes were used to detect the ROS and oxygen radical levels exhibited in JB6-AP-1 cells, respectively. Results indicated that NAC markedly inhibited ROS generation induced by TiO₂ NPs compared with the control (Fig. 3).

Cell viability. Following 24-h treatment with TiO₂ NPs alone, the MTT assay results indicated that the cell viability was significantly suppressed when compared with cells that were also treated with NAC (P<0.05; Fig. 4). Furthermore, the present findings demonstrated that the addition of NAC

significantly inhibited the cytotoxicity induced by TiO₂ NPs in JB6-AP-1 cells (P<0.05; Fig. 4).

AP-1 gene expression levels. AP-1 luciferase activity was significantly upregulated when cells were treated with 5, 10, 15, 20 and 25 $\mu\text{g}/\text{cm}^2$ of TiO₂ NPs alone compared with cells treated with the same concentration of TiO₂ NPs plus 40 nM NAC (P<0.05; Table II; Fig. 5). When cells were treated with 25 $\mu\text{g}/\text{cm}^2$ TiO₂ NPs, a reduced AP-1 luciferase activity level was exhibited when compared with cells treated with 20 $\mu\text{g}/\text{cm}^2$ TiO₂ NPs, which may be due to increased levels of apoptosis at this higher concentration (Table II, Fig. 5).

Discussion

Various types of NPs are under development for diagnostic and therapeutic applications in the biomedical field (18,19), yet knowledge about their possible toxicity in living cells remains limited (20). Furthermore, understanding on the prevention of NP toxicity in living cells is lacking. TiO₂ NPs have an extensive application in the industrial, food, cosmetics and medicine sectors. Previous results have demonstrated that TiO₂ NPs may be distributed in various organs and tissues in the body, following absorption through the gastrointestinal tract (21,22). In a previous study, it was demonstrated that TiO₂ NPs induced apoptosis in cultured JB6 cells (23). To investigate the underlying mechanism of the inhibition of NAC on the cytotoxicity induced by TiO₂ NPs, NP localization, ROS generation, cytotoxicity and AP-1 transcription factor regulation in JB6 cells transfected with the AP-1 gene treated with TiO₂ NPs alone or TiO₂ NPs plus NAC were evaluated in the present study.

The present results demonstrated that TiO₂ NPs, which were indicated to exhibit a mean core diameter of 42 nm, were transported into the cytoplasm once they had penetrated the cell membrane of JB6-AP-1 cells. No TiO₂ NPs were identified in the cell nucleus, which was indicated by a clear nuclear shadow and no observed FITC-fluorescence. Halamoda Kenzaoui *et al* (20) reported that following uptake by human brain-derived endothelial cells, TiO₂ NPs with a mean core diameter of 21 nm were transported into the lysosomes of these cells in the cytoplasm, which is in agreement with the present results. Gu *et al* (24) reported that gold NPs with an average diameter of 3.7 nm, which were modified with 3-mercaptopropionic acid and poly ethylene glycol, were able to penetrate into the nucleus of mammalian cells upon exposure for 24 h. Whether TiO₂ NPs have the ability to penetrate into the nucleus remains to be confirmed.

ROS are proposed to be associated with tumor metastasis, which is a complicated process involving migration, invasion of the tumor cells and angiogenesis (25). Generation of ROS is able to stimulate transcription by activating AP-1 and nuclear factor kappa B (26). Dhar *et al* (26) demonstrated that AP-1 activity abrogates transformation in JB6 cells, transgenic mice and human keratinocytes.

Wang *et al* (27) revealed that TiO₂ NPs exerted toxicity on murine spleen cells by promoting oxidative stress, which was indicated by the significantly increased levels of ROS in cells. Previous studies have suggested that oxidative stress may be induced by TiO₂ NPs in A549 cells and rat lung alveolar macrophages (28,29). Gurr *et al* (30) also reported that

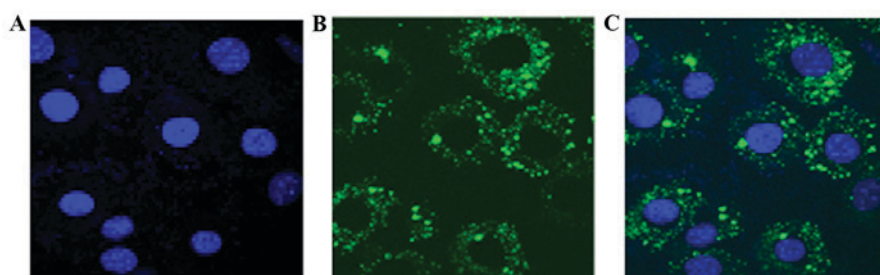


Figure 2. Localization of TiO₂ NPs in JB6-AP-1 cells. (A) Image of JB6-AP-1 cell nuclei stained with Hoechst 33342 (blue). (B) Fluorescein isothiocyanate-labeled TiO₂ NP staining (green dots) in JB6-AP-1 cells indicated localization of TiO₂ NPs in the cytoplasm. (C) A and B images merged. TiO₂ NPs, titanium dioxide nanoparticles. (magnification, x400).

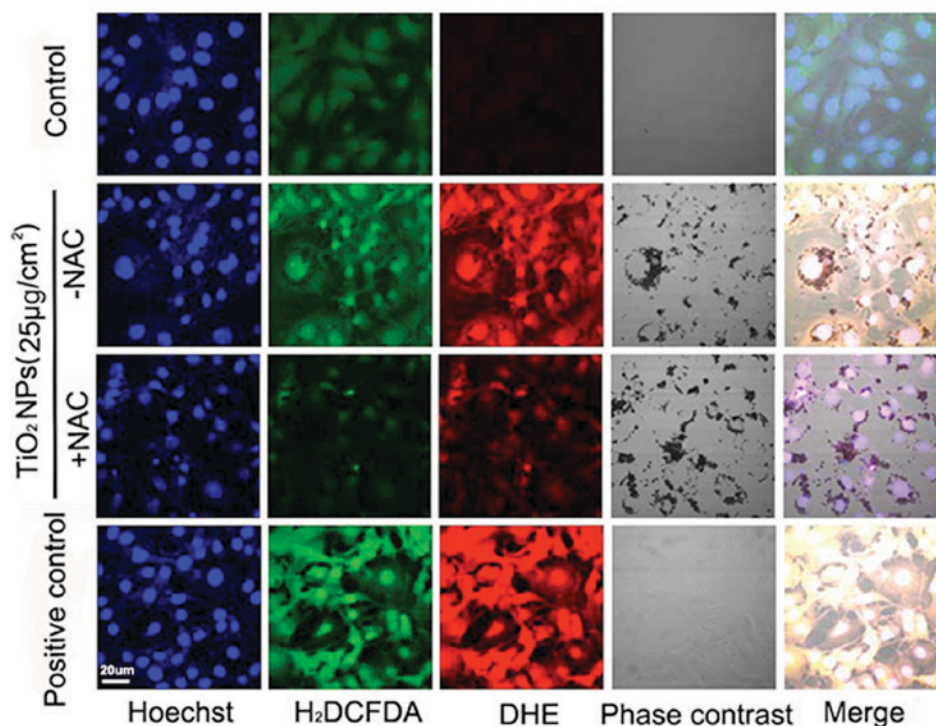


Figure 3. ROS detection. JB6-AP-1 cells were seeded onto a 24-well plate, incubated overnight and treated with 25 µg/cm² TiO₂ NPs with or without 40 nM NAC. The ROS generation was detected by H₂DCFDA and DHE staining. Cell apoptosis was detected by Hoechst staining (magnification x400). Phase contrast was used to locate the cells and images were merged to identify the position of ROSs in the nucleus and cytoplasm. ROS, reactive oxygen species; TiO₂ NPs, titanium dioxide nanoparticles; NAC, N-acetyl-cysteine; H₂DCFDA, 2',7'-dichlorodihydrofluorescein diacetate; DHE, dihydroethidium.

oxidative damage may be induced by TiO₂ NPs in BEAS 2B cells. Antioxidants are typically used to reduce free radical formation (31). Xue *et al* (32) indicated that NAC is able to inhibit ROS formation in cells exposed to TiO₂. Guo *et al* (33) observed in human umbilical vein endothelial cells that pretreatment with the free radical scavenger, NAC, inhibited the genotoxicity induced by multi-walled carbon nanotubes. Furthermore, in an *in vivo* study, El-Kirdasy *et al* (34) demonstrated the beneficial effect of NAC in preventing apoptosis in spermatogenic and sertoli cells, as well as alleviating testicular dysfunction induced by TiO₂ NPs in male albino rats.

In the present study, H₂DCFDA and DHE were used for staining general ROS or oxygen radicals produced in JB6-AP-1 cells, respectively (35). The present results demonstrated that treatment with TiO₂ NPs induced marked ROS generation in JB6-AP-1 cells. Fluorescence intensity indicated

that treatment with NAC inhibited both general ROS and oxygen radical levels induced by TiO₂ NPs and decreased the cytotoxicity of JB6-AP-1 cells. Furthermore, the luciferase assay revealed that NAC was able to downregulate AP-1 luciferase activity. These results suggest that the ability for NAC to inhibit the cytotoxicity induced by TiO₂ NPs and downregulate the gene expression levels of AP-1 in JB6-AP-1 cells may occur predominantly due to ROS scavenging. Furthermore, the present results suggest that NAC may be a useful antioxidant in preventing induced carcinogenesis by TiO₂ NPs. However, further *in vivo* studies are required to evaluate the effects of NAC in preventing induced toxicity by TiO₂ NPs.

In conclusion, the ability for NAC to inhibit cytotoxicity promoted by TiO₂ NPs may occur primarily through ROS scavenging in JB6-AP-1 cells. NAC is able to inhibit general ROS and oxygen radicals, as well as downregulate the luciferase activity of AP-1 gene expression. In addition, the present

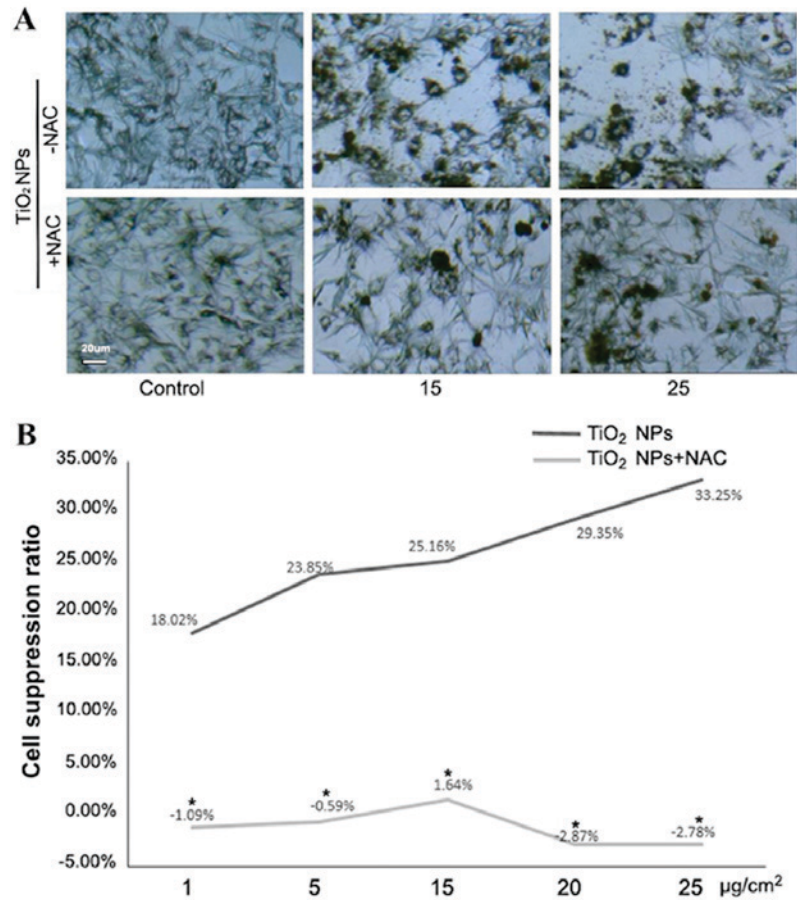


Figure 4. Cytotoxicity induced by TiO₂ NPs. The cell viability of JB6-AP-1 cells treated with varying concentrations (0, 1, 5, 15, 20 or 25 µg/cm²) of TiO₂ NPs with or without 40 nM NAC was detected by the MTT assay. (A) Cell morphological changes were captured under a light microscope (magnification, x400) and (B) the cell suppression ratio was calculated. Results indicated that cytotoxicity and cell apoptosis induced by TiO₂ NPs was significantly inhibited. *P<0.05 vs. control. TiO₂ NPs, titanium dioxide nanoparticles; NAC, N-acetyl-cysteine.

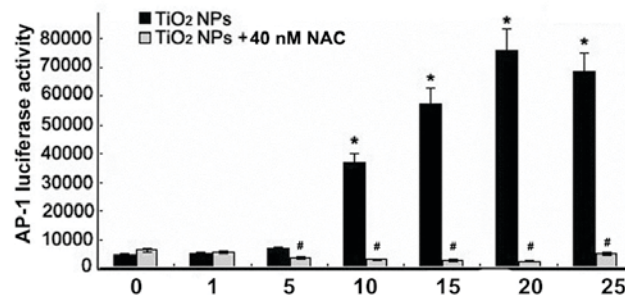


Figure 5. Relative AP-1 luciferase activity in JB6-AP-1 cells treated with varying concentrations (0, 1, 5, 10, 15, 20 or 25 µg/cm²) of TiO₂ NPs with or without 40 nM NAC (cells without any treatments were used as a control). NAC (40 nM) significantly downregulated the relative AP-1 luciferase activity that was upregulated by TiO₂ NPs. Data were analyzed using one-way analysis of variance. *P<0.05 vs. 0 µg/cm² TiO₂ NPs; #P<0.05 vs. TiO₂ NPs alone. AP-1, activator protein-1; TiO₂ NPs, titanium dioxide nanoparticles; NAC, N-acetyl-cysteine.

study demonstrated that TiO₂ NPs remained in the cytoplasm and did not penetrate the nuclear membrane.

Acknowledgements

The authors would like to thank Ms. Linda Bowman (Toxicology and Molecular Biology Branch, Health Effects Laboratory Division, National Institute for Occupational Safety

and Health, Morgantown, WV, USA) for her assistance in the preparation of this article. This study was partly supported by the National Nature Science Foundation of China (grant no. 81273111), the Scientific Projects of Zhejiang Province (grant nos. 2015C33148 and 2014C37117), Ningbo Scientific Innovation Team for Environmental Hazardous Factor Control and Prevention (2016C51001) and KC Wong Magna Fund in Ningbo University.

References

- Maynard AD (ed): *Nanotechnology: A research strategy for addressing risk*. 3rd edition. Woodrow Wilson International Center for Scholars, Washington, DC, pp7-17, 2006.
- Warheit DB, Sayes CM, Reed KL and Swain KA: Health effects related to nanoparticle exposures: Environmental, health and safety considerations for assessing hazards and risks. *Pharmacol Ther* 120: 35-42, 2008.
- Fujishima A, Rao TN and Tryk DA: Titanium dioxide photocatalysis. *J Photochem. Photobiol* 1: 1-21, 2000.
- Liu K, Lin X and Zhao J: Toxic effects of the interaction of titanium dioxide nanoparticles with chemicals or physical factors. *Int J Nanomedicine* 8: 2509-2520, 2013.
- Newman MD, Stotland M and Ellis JI: The safety of nanosized particles in titanium dioxide- and zinc oxide-based sunscreens. *J Am Acad Dermatol* 61: 685-692, 2009.
- Jacobs JJ, Skipor AK, Black J, Urban Rm and Galante JO: Release and excretion of metal in patients who have a total hip-replacement component made of titanium-base alloy. *J Bone Joint Surg Am* 73: 1475-1486, 1991.
- Trouiller B, Reliene R, Westbrook A, Solaimani P and Schiestl RH: Titanium dioxide nanoparticles induce DNA damage and genetic instability in vivo in mice. *Cancer Res* 69: 8784-8789, 2009.
- Wolf R, Matz H, Orion E and Lipozencic J: Sunscreens-the ultimate cosmetic. *Acta Dermatovenerol Croat* 11: 158-162, 2003.
- Hext PM, Tomenson JA and Thompson P: Titanium dioxide: Inhalation toxicology and epidemiology. *Ann Occup Hyg* 49: 461-472, 2005.
- Rajh T, Dimitrijevic NM and Rozhkova EA: Titanium dioxide nanoparticles in advanced imaging and nanotherapeutics. *Methods Mol Biol* 726: 63-75, 2011.
- Park S, Lee YK, Jung M, Kim KH, Chung N, Ahn EK, Lim Y and Lee KH: Cellular toxicity of various inhalable metal nanoparticles on human alveolar epithelial cells. *Inhal Toxicol* 19 (Suppl 1): S59-S65, 2007.
- Sha B, Gao W, Wang S, Xu F and Lu T: Cytotoxicity of titanium dioxide nanoparticles differs in four liver cells from human and rat. *Compos Part B Eng* 42: 2136-2144, 2011.
- De Flora S, Izzotti A, D'Agostini F and Balansky RM: Mechanisms of N-acetylcysteine in the prevention of DNA damage and cancer, with special reference to smoking-related end-points. *Carcinogenesis* 22: 999-1013, 2001.
- Childs A, Jacobs C, Kaminski T, Halliwell B and Leeuwenburgh C: Supplementation with vitamin C and N-acetyl-cysteine increases oxidative stress in humans after an acute muscle injury induced by eccentric exercise. *Free Radic Biol Med* 31: 745-753, 2001.
- Wang J, Deng X, Zhang F, Chen D and Ding W: ZnO nanoparticle-induced oxidative stress triggers apoptosis by activating JNK signaling pathway in cultured primary astrocytes. *Nanoscale Res Lett* 9: 117, 2014.
- Chen G, Shi J, Hu Z and Hang C: Inhibitory effect on cerebral inflammatory response following traumatic brain injury in rats: A potential neuroprotective mechanism of N-acetylcysteine. *Mediators Inflamm* 2008: 716458, 2008.
- Ding M, Zhao J, Bowman L, Lu Y and Shi X: Inhibition of AP-1 and MAPK signaling and activation of Nrf2/ARE pathway by quercitrin. *Int J Oncol* 36: 59-67, 2010.
- Liao SH, Liu CH, Bastakoti BP, Suzuki N, Chang Y, Yamauchi Y, Lin FH and Wu KC: Functionalized magnetic iron oxide/alginate core-shell nanoparticles for targeting hyperthermia. *Int J Nanomedicine* 10: 3315-3327, 2015.
- White-Schenk D, Shi R and Leary JF: Nanomedicine strategies for treatment of secondary spinal cord injury. *Int J Nanomedicine* 10: 923-938, 2015.
- Halamoda Kenzaoui B, Chapuis Bernasconi C, Guney-Ayra S and Juillerat-Jeanneret L: Induction of oxidative stress, lysosome activation and autophagy by nanoparticles in human brain-derived endothelial cells. *Biochem J* 441: 813-821, 2012.
- Xu J, Shi H, Ruth M, Yu H, Lazar L, Zou B, Yang C, Wu A and Zhao J: Acute toxicity of intravenously administered titanium dioxide nanoparticles in mice. *PLoS One* 8: e70618, 2013.
- Shi H, Magaye R, Castranova V and Zhao J: Titanium dioxide nanoparticles: A review of current toxicological data. *Part Fibre Toxicol* 10: 15, 2013.
- Zhao J, Bowman L, Zhang X, Vallyathan V, Young SH, Castranova V and Ding M: Titanium dioxide (TiO₂) nanoparticles induce JB6 cell apoptosis through activation of the caspase-8/Bid and mitochondrial pathways. *J Toxicol Environ Health A* 72: 1141-1149, 2009.
- Gu YJ, Cheng J, Lin CC, Lam YW, Cheng SH and Wong WT: Nuclear penetration of surface functionalized gold nanoparticles. *Toxicol Appl Pharmacol* 237: 196-204, 2009.
- Wu WS: The signaling mechanism of ROS in tumor progression. *Cancer Metastasis Rev* 25: 695-705, 2006.
- Dhar A, Young MR and Colburn NH: The role of AP-1, NF-kappaB and ROS/NOS in skin carcinogenesis: The JB6 model is predictive. *Mol Cell Biochem* 234-235: 185-193, 2002.
- Wang J, Li N, Zheng L, Wang S, Wang Y, Zhao X, Duan Y, Cui Y, Zhou M, Cai J, *et al*: P38-Nrf-2 signaling pathway of oxidative stress in mice caused by nanoparticulate TiO₂. *Biol Trace Elem Res* 140: 186-197, 2011.
- Scherbart AM, Langer J, Bushmelev A, van Berlo D, Haberzettl P, van Schooten FJ, Schmidt AM, Rose CR, Schins RP and Albrecht C: Contrasting macrophage activation by fine and ultrafine titanium dioxide particles is associated with different uptake mechanisms. *Part Fibre Toxicol* 8: 31, 2011.
- Jugan ML, Barillet S, Simon-Deckers A, Herlin-Boime N, Sauvaigo S, Douki T and Carriere M: Titanium dioxide nanoparticles exhibit genotoxicity and impair DNA repair activity in A549 cells. *Nanotoxicology* 6: 501-513, 2012.
- Gurr JR, Wang AS, Chen CH and Jan KY: Ultrafine titanium dioxide particles in the absence of photoactivation can induce oxidative damage to human bronchial epithelial cells. *Toxicology* 213: 66-73, 2005.
- Fiedor J and Burda K: Potential role of carotenoids as antioxidants in human health and disease. *Nutrients* 6: 466-488, 2014.
- Xue C, Liu W, Wu J, Yang X and Xu H: Chemoprotective effect of N-acetylcysteine (NAC) on cellular oxidative damages and apoptosis induced by nano titanium dioxide under UVA irradiation. *Toxicol In Vitro* 25: 110-116, 2011.
- Guo YY, Zhang J, Zheng YF, Yang J and Zhu XQ: Cytotoxic and genotoxic effects of multi-wall carbon nanotubes on human umbilical vein endothelial cells in vitro. *Mutat Res* 721: 184-191, 2011.
- El-Kirdasy AF, Nassan MA, Baiomy AAA, Ismail TA, Soliman MM and Attia HF: Potential ameliorative role of n-acetylcysteine against testicular dysfunction induced by titanium dioxide in male albino rats. *Am J Pharmacology Toxicology* 9: 29-38, 2014.
- Zhao J, Bowman L, Magaye R, Leonard SS, Castranova V and Ding M: Apoptosis induced by tungsten carbide-cobalt nanoparticles in JB6 cells involves ROS generation through both extrinsic and intrinsic apoptosis pathways. *Int J Oncol* 42: 1349-1359, 2013.